Propagating Long Waves on Oceanic Density Fronts: An Analytic Model

RICHARD W. GARVINE

College of Marine Studies, University of Delaware, Newark, DE 19716

ABSTRACT

An analytic model of long, propagating free-wave perturbations to an established upper ocean density front is developed. The primary purpose of the model is to illuminate basic frontal wave mechanisms for possible subsequent use in more sophisticated numerical models. The model is of the barotropic class but has ageostrophic dynamics because of the basic state adopted, essentially Stommel's model of the Gulf Stream with uniform potential vorticity and order one Rossby number. The model assumes inviscid dynamics apart from a narrow dissipative zone adjacent to the surface front. The latter exerts a bulk effect on the larger inviscid zone, especially in generating small, but finite, cross-stream flow in the basic state. For zero cross-flow the resulting waves are stable, have downstream phase speeds that are slow compared to the current speed and that increase with frequency, and have anomalous dispersion. The phase speeds compare well with the analysis of observations of propagating Gulf Stream meanders by Halliwell and Mooers. For finite cross-flow the waves grow slowly in the downstream direction when flow is out of the current and decay when flow is into the current. The rates of growth or decay are independent of wavelength. Corresponding net growth or decay in the wave kinetic energy is produced by action of the cross-correlation wave Reynolds stress against the lateral shear of the basic state current.

1. Introduction

Wave perturbations to upper ocean density fronts are common mesoscale features, best known from decades of observations of the Gulf Stream front downstream of Cape Hatteras where they have been called meanders. Their major properties are low subinertial frequencies and long wavelengths. For the Gulf Stream typical ratios of downstream wavelength to width of the basic current are about 10 (Halliwell and Mooers, 1983). Perhaps most puzzling is the slowness of the observed phase speeds, typically only a few percent of the basic current speed. These waves also show a strong tendency toward downstream spatial growth over scales comparable to the wavelength itself. Further background, including an extended discussion of previous models of related wave dynamics, is given in my recent paper on the subject (Garvine, 1983; hereafter termed G83).

The model I develop here is an extension of G83 and has the following seven major characteristics:

1) The model is effectively barotropic in that only the upper layer of uniform buoyancy is active; this restriction is in contrast to baroclinic models, such as Orlanski's (1969) where upper and lower layers are both active and coupled.

2) The undisturbed or basic state is a simple extension of Stommel's (1966, p. 112) model of the Gulf Stream. The potential vorticity P is assumed to be uniform. Stommel reasoned that since observations of the source water for the Gulf Stream in the western

Atlantic showed nearly uniform P, its subsequent advection into the current where inertial effects dominate should yield a current of uniform P, also. Very recently this reasoning has been significantly supported and strengthened by the theoretical work of Rhines and Young (1982a,b). Indeed, maps of P presented by McDowell *et al.* (1982) for water above the thermocline but below the direct reach of atmospheric influence show remarkable uniformity over the wind gyre of the North Atlantic.

3) As a consequence of (2), the model has ageostrophic dynamics, because the strong downstream frontal jet of the basic state has a Rossby number of $O(1)$, i.e., relative and planetary vorticities are of the same order.

4) The upper layer flow is taken as inviscid apart from a narrow, dissipative zone adjacent to the surface front. There, however, local turbulence production is likely, so that P cannot be conserved along streamlines. Johns and Watts (1982) show a vertical section of P contours across the Gulf Stream downstream of Cape Hatteras which displays little change in P above the thermocline except for a small area near the surface front roughly coincident with cyclonic shear in the downstream current. Assaf (1977) developed a steady-state model for the Florida Current where vertical, interfacial friction operated wherever the local densimetric Froude number exceeded a threshold value. His numerical calculations showed realistic cyclonic shear zone structure. Here the basic concept of Assaf's model is employed, but not the

details, since they would prevent analytic description, even in a steady state. Instead, as in G83, I stipulate that wave perturbations merely displace or wrinkle the inner dissipative zone without otherwise altering its structure. Its bulk effect on the outer, inviscid zone appears as constraints on interface depth and cross-stream velocity at the common boundary. Its primary influence is the imposition of a small, cross-stream basic state current upon the inviscid zone required to balance the flux of mass across the frontal interface in the dissipative zone induced by turbulent entrainment.

5) The basic state in general has a small cross-stream current $\bar{u}$, a result of this entrainment. For $\bar{u} = 0$ waves are stable, but for $\bar{u} > 0$ they grow downstream, while for $\bar{u} < 0$ they decay.

6) Only linear (small amplitude) waves are treated.

7) The model is developed for the long wave limit only.

In G83 I treated a similar problem. This paper, however, differs in three important ways. First, here I treat $\bar{u} \neq 0$, whereas in G83 $\bar{u} = 0$. Second, here I relax the stipulation of G83 that shear in the locally parallel velocity vanish at the boundary between the dissipative and inviscid zones. In G83 this constraint permitted only stationary waves, that is, steady state meanders with zero phase speed. Here the small shear permitted allows propagating waves. Third, here I treat only the long wave limit and thereby obtain simple, analytic solutions, whereas in G83 I treated arbitrary wavelength but had to obtain solutions numerically.

Martin (1981) developed a numerical model with similar characteristics to those above. In applications to the Gulf Stream front he found slow, downstream wave propagation and sharp changes in rates of wave energy growth with $\bar{u}$ having fastest growth for $\bar{u} > 0$. Paldor (1982) developed a similar model to G83 having uniform P and $\bar{u} = 0$, but he assumed inviscid flow up to and including the surface front. Using a Rayleigh integral, he proved that this flow was stable for small perturbations of any wavelength.

Section 2 presents the model development, section 3 the basic state, and section 4 the perturbation equations. Section 5 then gives the wave properties when $\bar{u} = 0$ and section 6 for $\bar{u} \neq 0$. Section 7 concludes the paper.

2. Model development

Figure 1 shows a schematic of the model geometry in its basic (unperturbed) state. Two incompressible layers are treated, a deep ambient water layer of uniform density ρ_∞, and a light water layer above the frontal interface of uniform density $\rho_\infty - \Delta\rho$. The depth of the latter is d^* which vanishes at the surface front. (Asterisks denote dimensional variables.) The source of the light water is called the parent pool

where the depth is given as d_b^*. Within the parent pool the potential vorticity is uniform and given by $P^* = f/d_b^*$, where f is the Coriolis parameter.

The model will be limited in application to upper ocean density fronts where the flow is inviscid apart from a narrow region near the surface front termed the dissipative zone (Fig. 1) where $d^* < d_b^*$. The dissipative zone represents the domain where locally high turbulence production is expected from such processes as mean vertical shear instability owing to locally high densimetric Froude numbers, or, equivalently, low gradient Richardson numbers. In this domain, in contrast to the inviscid zone, potential vorticity will not be conserved along particle paths. Instead, the locally high vertical friction will generate cyclonic horizontal shear, as in the steady state models of Assaf (1977), Kao (1980) and Garvine (1980) for the Gulf Stream front. In addition, vertical volume flux by turbulent entrainment across the frontal interface in the dissipative zone will force horizontal volume flux across the inviscid zone into or out of the parent pool, depending on the net entrainment direction in the dissipative zone.

Small amplitude free wave disturbances will be imposed upon the basic state. In the inviscid zone these will be determined analytically by solving the perturbation equations using an asymptotic expansion for small wavenumber. In the dissipative zone no explicit solution will be attempted for the perturbations, because even the basic state there is too complicated for analytic solution. Instead, as in G83, I will stipulate that wave perturbations will merely displace the dissipative zone without otherwise altering its structure. Its bulk effect on the larger inviscid zone will, nevertheless, be accounted for by inner boundary conditions on the interface depth and cross-stream velocity at the common boundary, termed the inner boundary (Fig. 1). The primary effect of the dissipative zone will be the generation of a source or sink of cross-stream volume flux, which, in turn, will affect fundamentally the stability of the waves in the whole domain.
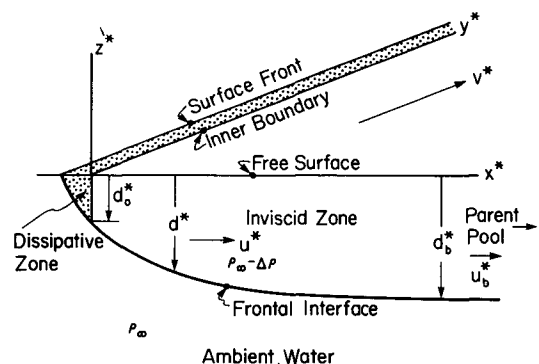

FIG. 1. Schematic cross section of the model front.

Standard oceanographic model restrictions are imposed. The Boussinesq approximation is assumed valid, wind stress is neglected, vertical gradients in horizontal current in the inviscid zone are absent, and beta effects are neglected. The upper layer is assumed shallow compared to the water depth, so that the upper layer pressure field is in isostatic equilibrium. The ambient water is taken to be at rest and the front to have zero mean velocity of propagation normal to itself; these latter restrictions may be removed following G83, but have no fundamental effect on the properties of the frontal waves or their stability.

The independent variables are the time t^*, the cross-stream distance x^* (Fig. 1), and the downstream distance y^*; u^* and v^* are the corresponding velocity components and the potential vorticity is P^*. Following G83 I introduce scaled variables as

$$(x, y) = \frac{(x^*, y^*)}{\lambda}, \quad t = ft^*, \quad (u, v) = \frac{(u^*, v^*)}{c_i},$$

$$d = \frac{d^*}{d_b^*} \quad P = \frac{P^* d_b^*}{f},$$

where $c_i = (g'd_b^*)^{1/2}$ with $g' = g\Delta\rho/\rho_\infty$, the reduced gravity, so that c_i is the linear internal wave velocity and $\lambda = c_i/f$, the internal Rossby radius. As these scaled variables imply, c_i is the scale for the current, λ for the cross-stream distance, and f/d_b^* for the potential vorticity.

In these scaled variables the governing equations of potential vorticity, cross-stream, and downstream momentum are, respectively (G83):

$$\frac{DP}{Dt} = 0, \tag{1}$$

$$\frac{Du}{Dt} - v + \frac{\partial d}{\partial x} = 0, \tag{2}$$

$$\frac{Dv}{Dt} + u + \frac{\partial d}{\partial y} = 0, \tag{3}$$

where $D/Dt \equiv \partial/\partial t + u\partial/\partial x + v\partial/\partial y$, the material derivative, and $P \equiv (\partial v/\partial x - \partial u/\partial y + 1)/d$. Here (1) states the conservation of potential vorticity along particle trajectories and will be used as an alternate to the continuity equation.

3. The basic state

The flow state is decomposed in standard fashion into a basic state that represents the steady, undisturbed flow and a perturbation, here assumed small. Thus,

$$u = \bar{u} + u', \quad v = \bar{v} + v', \quad d = \bar{d} + d', \quad P = \bar{P} + P', \tag{4}$$

where overbars denote basic state and primes perturbation variables.

As in G83, the essential model physics arises from the assumption of uniform potential vorticity for the basic state in the parent pool and, thus, for the entire inviscid zone as well, an idea Stommel (1966) was first to postulate. Consequently, $\bar{P} = 1$. Since I further assume the front is straight and parallel to y in the basic state, $\partial/\partial y \ll \partial/\partial x$. As shown in G83, the solutions for $\bar{d}$ and $\bar{v}$ for the inviscid zone without cross-stream flow ($\bar{u} = 0$) are then

$$\bar{d} = 1 - v_0 e^{-x}, \quad \bar{v} = 1 - \bar{d} = v_0 e^{-x}, \tag{5}$$

where $v_0 = 1 - d_0$ with d_0 the scaled depth at the inner boundary. Equations (5) are the same as Stommel (1966, p. 111) obtained, except here $v_0 \leq 1$, i.e., the frontal interface need not surface at the inner boundary ($d_0 \geq 0$).

Small, but finite, basic state cross-stream volume flux in the inviscid zone will be generated by mass entrainment in the dissipative zone. Within the inviscid zone this volume flux is uniform so that in the absence of y-derivatives, we have from mass continuity $\bar{u}^*\bar{d}^* = u_b^* d_b^*$ where u_b^* is the (dimensional) cross-stream flow into the parent pool. For convenience, let this be represented by

$$u_b^* = c_i S_e F,$$

where S_e denotes the sign of the entrainment ($S_e = +1$ for entrainment into the upper layer and $S_e = -1$ for entrainment into the ambient layer) while $F \equiv |u_b^*|/c_i$ is the Froude number indicating the relative speed of the outflow (or inflow). In contrast to small-scale density fronts where $F = O(1)$ (Garvine, 1974; Kao et al., 1977), for the large scale fronts of interest here $F \ll 1$, typically 10^{-2}. With this nomenclature we then have

$$\bar{u} = S_e F/\bar{d}. \tag{6}$$

It may be shown that $\bar{u}$ alters the basic state solution of (1)–(3) only at $O(F^2)$. Because I will include only terms through $O(F)$ subsequently, (5) will still be valid for $\bar{d}$ and $\bar{v}$.

The Froude number F will emerge as the small parameter associated with frontal wave stability. The basic state of G83, in contrast, assumed $\bar{u} = 0$ (or $F = 0$) and was associated with only stable waves.

4. The perturbation equations

Substitution of the decomposition forms (4) into the governing equations (1)–(3) and retention of only first order perturbation terms yields the inviscid zone linear perturbation equations. The perturbation potential vorticity equation is especially simple, since (1) dictates conservation of P following the fluid, while $\bar{P} = 1$ by postulate. Thus, $P' = 0$ everywhere in the inviscid zone, yielding

$$\frac{\partial v'}{\partial x} - \frac{\partial u'}{\partial y} - d' = 0. \tag{7}$$

The perturbation x- and y-momentum equations are

$$\frac{\partial u'}{\partial t} + \bar{v}\frac{\partial u'}{\partial y} - v' + \frac{\partial d'}{\partial x} + S_e F \frac{\partial}{\partial x}\left(\frac{u'}{\bar{d}}\right) = 0, \quad (8)$$

$$\frac{\partial v'}{\partial t} + \bar{v}\frac{\partial v'}{\partial y} + \left(1 + \frac{d\bar{v}}{dx}\right)u' + \frac{\partial d'}{\partial y} + \frac{S_e F}{\bar{d}}\frac{\partial v'}{\partial x} = 0. \quad (9)$$

Note the appearance in (8) and (9) of both downstream advection terms, with $\bar{v}(x)$ as a factor, as well as cross-stream advection terms containing $S_e F/\bar{d} = \bar{u}$; these latter terms bring the small parameter F into the problem.

Following G83, I adopt the wave forms

$$u'(x, y, t) = -i[X_0(x) + iFX_1(x)]e^{i\phi}, \quad (10a)$$

$$v'(x, y, t) = [Y_0(x) + iFY_1(x)]e^{i\phi}, \quad (10b)$$

$$d'(x, y, t) = [Z_0(x) + iFZ_1(x)]e^{i\phi}, \quad (10c)$$

where $i = \sqrt{-1}$ and ϕ is the phase function given by

$$\phi(y, t) \equiv (k - iF\kappa)y - \omega t. \quad (10d)$$

In evaluating any of the perturbation variables the real part must be taken. Here k is the scaled wavenumber, taken as real, while ω is the scaled wave frequency, shown later to be real, and κ anticipates the possibility of wave instability ($\kappa > 0$) or decay ($\kappa < 0$) when the wavenumber has an imaginary part for small, but finite, F. The wave forms anticipate that u' will be in quadrature phase with v' and d' when $F = 0$, while a primary effect of $F > 0$ will be to change the relative phases of the variables. The eigenfunctions $X_0(x)$, $X_1(x)$, $Y_0(x)$, etc. will all turn out to be real. Subscripts "0" denote the eigenfunctions for the limiting case of $F = 0$ (no cross-flow in the basic state) while subscripts "1" denote corrections for F small but finite.

Substitution of the wave forms (10) into the perturbation equations (7)–(9) and retention of only $O(1)$ terms yields the following zeroth order system of ordinary differential equations.

$$\frac{dY_0}{dx} - kX_0 - Z_0 = 0, \quad (11a)$$

$$(k\bar{v} - \omega)X_0 - Y_0 + \frac{dZ_0}{dx} = 0, \quad (11b)$$

$$(k\bar{v} - \omega)Y_0 - \left(1 + \frac{d\bar{v}}{dx}\right)X_0 + kZ_0 = 0. \quad (11c)$$

These are identical in form to (14) of G83 with $\omega = 0$.

Retaining terms through $O(F)$ yields the first order system.

$$\frac{dY_1}{dx} - kX_1 - Z_1 = -\kappa X_0, \quad (12a)$$

$$(k\bar{v} - \omega)X_1 - Y_1 + \frac{dZ_1}{dx} = \kappa\bar{v}X_0 + S_e \frac{d}{dx}\left(\frac{X_0}{\bar{d}}\right), \quad (12b)$$

$$(k\bar{v} - \omega)Y_1 - \left(1 + \frac{d\bar{v}}{dx}\right)X_1 + kZ_1$$
$$= \kappa(\bar{v}Y_0 + Z_0) + \frac{S_e}{\bar{d}}\frac{dY_0}{dx}. \quad (12c)$$

The left sides of these are identical to (11), but inhomogenous or forcing terms now appear on the right generated by the coupling of finite cross-flow and downstream wave amplitude growth or decay to the $F = 0$ wave field.

5. Long waves without cross-stream flow

In this section I treat long waves without cross-stream flow in the basic state, i.e., in the limits $k^2 \ll 1$ and $F = 0$ (or $\bar{u} = 0$). The system to be solved is (11) for $k^2 \ll 1$ subject to the boundary conditions for frontal "trapped" waves

$$X_0, Y_0, Z_0 \rightarrow 0, \quad \text{for} \quad x \rightarrow \infty, \quad (13)$$

and to those at the displaced inner boundary where $x = h(y, t)$. The inner boundary displacement may be written, consistent with the wave forms (10), as

$$h(y, t) = He^{i\phi},$$

where H is the frontal displacement amplitude. The inner boundary conditions I impose, as in G83, are that the interface depth at the displaced inner boundary is unchanged from that of the basic state, d_0, while the fluid velocity component locally normal to the boundary is likewise unchanged. For $\bar{u} = 0$ these are (G83), respectively:

$$Z_0(0) = -v_0 H = -1, \quad (14a)$$

$$X_0(0) = -kv_0 H + \omega H = -k + \omega/v_0, \quad (14b)$$

where $v_0 H$ is equated to unity for convenience, since the particular amplitude of a free wave may be chosen arbitrarily.

The mathematical problem then is to solve the system (11) subject to the boundary conditions (13) and (14). This is nearly the same problem as in G83, but with two important differences. First, the stipulation of G83 that there be no shear of the locally parallel velocity component at the inner boundary is relaxed, i.e., now only the normal component must match that of the (unchanged) dissipative zone. Second, an asymptotic expansion is employed yielding analytic solutions through $O(k^2)$ for $k^2 \ll 1$. The first difference permits the existence of propagating, as opposed to stationary, waves, while the second provides simple, analytic solutions in a limit of primary physical interest.

If one stipulates that the dissipative zone is merely displaced by the wave perturbations, but is otherwise unaltered as here and in G83, and also stipulates the no shear condition as in G83, then one has

$$Y_0(0) = v_0 H = 1. \quad (15)$$

If this is inserted, together with the inner boundary conditions (14), into the y-momentum equation (11c) and evaluated at $x = 0$, one finds $\omega = 0$ for all k, i.e., only stationary or steady state waves are possible, as in G83. Conversely, relaxing the no-shear stipulation, as here, permits $\omega \neq 0$ or propagating waves.

Appropriate asymptotic expansions for the long wave limit are

$$\left.\begin{array}{l} X_0(x) = k[R_0^{(0)}(x) + k^2 R_0^{(1)}(x) + \cdots] \\[6pt] Y_0(x) = Y_0^{(0)}(x) + k^2 Y_0^{(1)}(x) + \cdots \\[6pt] Z_0(x) = Z_0^{(0)}(x) + k^2 Z_0^{(1)}(x) + \cdots \end{array}\right\} \quad . \quad (16)$$

Here k^2 is the small expansion parameter, while all eigenfunctions on the right, including $R_0^{(0)}$ and $R_0^{(1)}$, are $O(1)$. These forms thus anticipate that X_0 (or u') will be $O(k)$, while Y_0 (or v') and Z_0 (or d') will be $O(1)$.

Substituting (16) into (11), assuming that $\omega = O(k^m)$ with $m > 1$, and retaining only the zeroth order terms in k^2 yields

$$dY_0^{(0)}/dx - Z_0^{(0)} = 0, \quad (17a)$$

$$-Y_0^{(0)} + dZ_0^{(0)}/dx = 0, \quad (17b)$$

$$\bar{v}Y_0^{(0)} - (1 + d\bar{v}/dx)R_0^{(0)} + Z_0^{(0)} = 0. \quad (17c)$$

Equation (17a) indicates that potential vorticity changes are absent as a result of a balance between the perturbations in lateral shear and interface depth, while (17b) indicates the cross-stream momentum balance to this order is geostrophic. This pair may be solved easily and the boundary conditions (13) and (14a) imposed to give

$$Y_0^{(0)}(x) = -Z_0^{(0)}(x) = e^{-x}. \quad (18)$$

Thus, at this order of approximation, $Y_0^{(0)}$ satisfies (15), indicating zero shear of the parallel velocity across the inner boundary.

The downstream momentum equation (17c) may now be solved easily to yield

$$R_0^{(0)}(x) = \frac{X_0^{(0)}(x)}{k} = -e^{-x}. \quad (19)$$

This identically satisfies the boundary condition (14b) to zeroth order.

The simplicity of (17c) and its solution (19), however, masks a complicated downstream momentum balance between four of the six terms of the perturbation equation (9): downstream advection by the basic state ($\bar{v}\partial v'/\partial y$), the Coriolis term ($u'$), cross-stream advection by the perturbations ($u'd\bar{v}/dx$), and the perturbation pressure gradient ($\partial d'/\partial y$). Consequently, (17c) is highly ageostrophic, reflecting the $O(1)$ Rossby number of the basic state, and lacks only the local acceleration term and cross-stream advection by the basic state of (9).

The first order equations in k^2 are

$$dY_0^{(1)}/dx - Z_0^{(1)} = R_0^{(0)}, \quad (20a)$$

$$-Y_0^{(1)} + dZ_0^{(1)}/dx = -\bar{v}R_0^{(0)}, \quad (20b)$$

$$\bar{v}Y_0^{(1)} - (1 + d\bar{v}/dx)R_0^{(1)} + Z_0^{(1)} = (\omega/k^3)Y_0^{(0)}. \quad (20c)$$

This system differs from the zeroth order one in three ways: the cross-stream flow now participates in the vorticity balance of (20a), downstream advection of momentum by the basic state renders even the cross-stream momentum balance ageostrophic in (20b), and the local acceleration is added to the downstream momentum balance in (20c). The latter represents the only time dependent term in the governing equations to first order and brings ω into the problem. Consistency requires $\omega = O(k^3)$ or $m = 3$.

Equations (20a) and (20b) may be solved for $Y_0^{(1)}$ and $Z_0^{(1)}$ subject to (13) and the boundary condition $Z_0^{(1)}(0) = 0$, consistent with (14a), to yield

$$Z_0^{(1)}(x) = \frac{2}{3} v_0 e^{-x}(1 - e^{-x}) + \frac{1}{2} x e^{-x}, \quad (21a)$$

$$Y_0^{(1)}(x) = \left(\frac{1}{2} - \frac{2}{3} v_0\right)e^{-x} + \frac{1}{3} v_0 e^{-2x} - \frac{1}{2} x e^{-x}. \quad (21b)$$

If (20c) is now solved for $R_0^{(1)}$ and evaluated at $x = 0$ one finds,

$$R_0^{(1)}(0) = \frac{v_0}{6d_0}(3 - 2v_0) - \frac{\omega}{d_0 k^3}.$$

However, the boundary condition (14b), if evaluated to $O(k^2)$, gives

$$R_0^{(1)}(0) = \frac{\omega}{v_0 k^3}.$$

Equating these gives the dispersion relation

$$\omega = \frac{v_0^2}{6}(3 - 2v_0)k^3. \quad (22)$$

Since k is small and $\omega = O(k^3)$, these waves have low subinertial frequencies and slow phase speeds. Because the waves are so slow, their corresponding downstream fluid acceleration $\partial v'/\partial t$ enters the downstream momentum balance only at $O(k^2)$, so that the solutions to this order, as well as to $O(1)$, must be found in order to determine ω.

For the limit of vanishing dissipative zone ($d_0 \rightarrow 0$ or $v_0 \rightarrow 1$) $\omega \rightarrow k^3/6$. This limit agrees with Paldor's (1982) analysis of his model for long waves, as expected, since Paldor's model assumed inviscid flow everywhere ($d_0 = 0$). For small d_0 the more general result of (22) is quite close to the limiting value; for example, when $d_0 = 0.1$ (or $v_0 = 0.9$), (22) gives $\omega = 0.162k^3$, a difference of less than 3% from the limiting case.

The phase and group velocities derived from (22) are

$$c = \frac{\omega}{k} = \frac{v_0^2}{6}(3 - 2v_0)k^2, \qquad (23a)$$

$$c_g = \frac{\partial \omega}{\partial k} = 3c. \qquad (23b)$$

Since $c_g > c$, these waves have anomalous dispersion. They propagate only downstream with phase speeds of $O(k^2)$, i.e., much slower than the downstream current speed. Martin (1981) developed a numerical model of frontal waves which featured a single, active, upper layer and a dissipative zone that also was advected by frontal displacements, but otherwise unchanged, as here. His basic state structure was also similar. He imposed a half-wave sinusoidal displacement to the basic state, simulating a trough, and computed the subsequent evolution of the flow. The particular case most related to the present model had an equivalent value of $k^2 = 0.147$, within the long wave limit, $kH = 0.105$ (small amplitude), $F = 0$, and $v_0 = \frac{2}{3}$. He found downstream propagating waves of normalized phase speed $c = 0.0334$, while (23a) gives $c = 0.0181$, somewhat slower. He also found that shorter waves developed downstream of the initial wave which had higher phase speeds, implying anomalous dispersion behavior, as in the present model.

The low speed of long waves (meanders) of the Gulf Stream compared to the swiftness of the current has been often remarked (Hansen, 1970; Halliwell and Mooers, 1983). Comparison of present results with observations of deep water Gulf Stream meander properties is therefore of interest, though such comparisons must be made cautiously, because the ratio of upper layer to total depth is not very small, about 1/5.

The most comprehensive observational data set for deep water Gulf Stream meanders is that of Halliwell and Mooers (1983). They analyzed meander properties from a four-year collection of weekly charts derived from satellite infrared images for the region up to 1000 km downstream of Cape Hatteras and found two dominant modes: very low-frequency standing waves with periods of months to years and downstream propagating waves with periods of several weeks. The present results pertain to the latter, propagating mode.

First, I compare results for one particular case and then the phase speeds and wavelengths over a wide frequency range. To compute dimensional values from the present results for comparison, the variables must be unscaled. I selected as typical of the Gulf Stream $f = 9 \times 10^{-5}$ s^{-1} (39°N) and $c_i = 2.5$ m s^{-1}, corresponding to a mean density difference of $\Delta\rho/\rho_\infty = 7 \times 10^{-4}$ and a pycnocline depth $d_b^* = 900$ m; consequently the Rossby radius is $\lambda = 27.8$ km. For simplicity I took $d_0 = 0$ ($v_0 = 1$). The model then gives

$$c^* = 1.87c_i(\Omega/f)^{2/3}, \qquad (24a)$$

$$\Lambda = 1.87\lambda(\Omega/f)^{-1/3}, \qquad (24b)$$

where c^* is the dimensional phase velocity, Λ the dimensional wavelength, and $\Omega \equiv 1/T^*$, the reciprocal period. For $\Omega = 8$ cycles/year (cpy), Halliwell and Mooers (1983) found for the most energetic waves values of $c^* = 9.1$ cm s^{-1} and $\Lambda = 360$ km; the model gives $c^* = 9.3$ cm s^{-1} and $\Lambda = 369$ km, corresponding to $c = 0.0373$ and $k^2 = 0.224$. They roughly estimated the group velocity c_g^* for the frequency band 4 to 10 cpy at 17 cm s^{-1}, while the model gives 28 cm s^{-1}. Results for c^* and Λ are compared in Fig. 2. The model gives $c^* \alpha \Omega^{2/3}$ and agrees well with both the trend and the particular values of the observations. Alternatively, one may compare values of Λ, although these are not independent of c^*, since $\Lambda = c^*/\Omega$. Values of $\Omega > 10$ cpy were not compared because $k^2 > 0.26$ then, so that the long wave limit is dubious.

In essence, the observations and model results have the following common features: comparable, slow phase speeds for given frequency, increasing phase speeds with increasing frequency, and anomalous dispersion ($c_g^* > c^*$). This agreement suggests that the model provides a simple, "lowest order" description of such waves in the same sense that Stommel's (1966) model, used here for the basic state, does for the mean Gulf Stream downstream of Cape Hatteras.

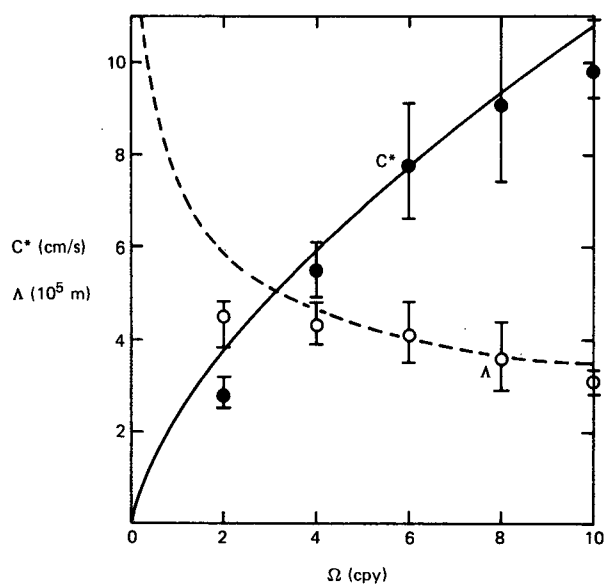The scaled eigenfunctions X_0, Y_0, and Z_0, com-

FIG. 2. Comparison of the observational results from Halliwell and Mooers (1983) and the present model for wave phase speed c^* and wavelength Λ for wave frequency Ω up to 10 cycles/year. Circles denote the values for the most energetic waves and the brackets the associated 95% confidence intervals from Halliwell and Mooers.

puted through $O(k^2)$, as well as their $O(1)$ parts are plotted versus x in Fig. 3 for the particular case above where $d_0 = 0$ and $k^2 = 0.224$. Note that the $O(k^2)$ corrections are modest even for this relatively large k^2. The trapped character of the waves is evident in the clear exponential decay for large x. One may more readily interpret the eigenfunctions by taking the real parts of the wave forms (10) to give, for $F = 0$,

$$u' = X_0 \sin \phi, \quad v' = Y_0 \cos \phi,$$

$$d' = Z_0 \cos \phi, \quad h = H \cos \phi,$$

where $\phi(y, t)$ is the phase function given by (10d). Since $Y_0 \geq 0$, the downstream wave velocity v' is in phase with the frontal displacement h, so that at wave troughs ($h = H$ or maximum frontal displacement toward the parent pool) the downstream flow is faster than the basic state, while at wave crests ($h = -H$) it is slower. Conversely, since $Z_0 \leq 0$, the interface displacement d' is out of phase with both h and v', so that the interface shoals at the wave troughs but deepens at the crests: A property which should be
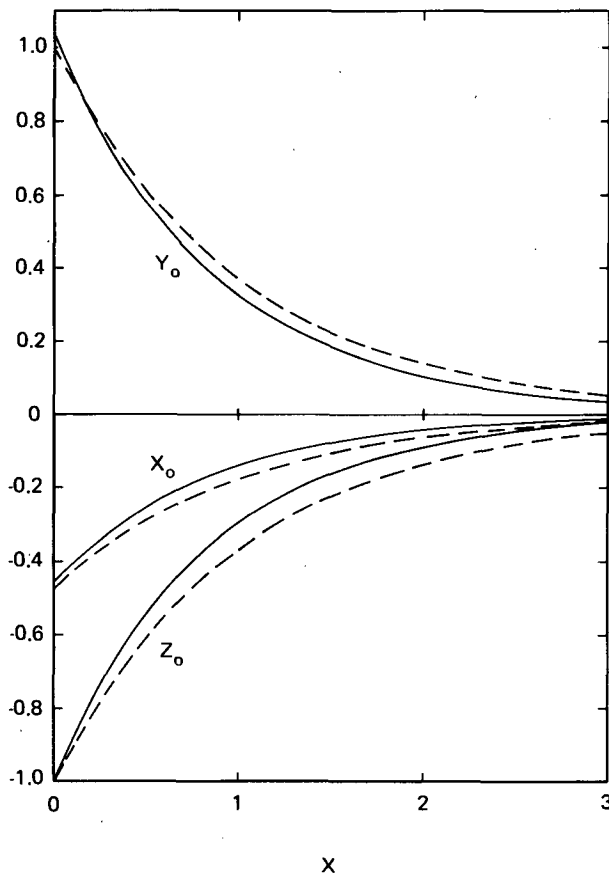
readily observable in frontal wave hydrography. In contrast u' is in quadrature phase with h, v', and d', having maximum values where $h = 0$ and zero values at troughs and crests. The quadrature phase with v' means that the Reynolds stress, the mean of $-u'v'$ over a period, will vanish, consistent with stable waves.

The velocity shear across the inner boundary may be expressed, following (14) and (20c), as

$$k^2 Y_0^{(1)}(0) \cos\phi = k^2 \cos\phi(\omega/k^3 v_0) = c \cos\phi/v_0.$$

If this shear were required to vanish for all y and t, as in G83, then $\omega = 0 = c$, and the waves would be steady and stationary, as in G83. There the long wave limit, $k^2 \rightarrow 0$, corresponded to only a trivial solution for the zeroth wave mode. All nontrivial, higher wave modes had $k^2 \geq O(1)$, so that no long waves were possible. The present results may therefore be viewed as an extension of G83 for the zeroth mode or long wave limit.

6. Long waves with slow cross-stream current

I treat in this section long waves with slow cross-stream current in the basic state, i.e., $k^2 \ll 1$ with $0 < F \ll 1$ (or $\bar{u} \neq 0$). The wave forms are given by (10) where the eigenfunctions to be found now are $X_1(x)$, $Y_1(x)$, and $Z_1(x)$, while the governing equations are given by (12). The boundary conditions are that the eigenfunctions vanish for $x \rightarrow \infty$, as in (13) for the $F = 0$ flow, and that the interface depth and locally normal fluid velocity at the displaced inner boundary match that of the adjacent dissipative zone. The latter conditions are extensions of (14) and may be written

$$Z_1(0) = 0, \tag{25a}$$

$$X_1(0) = \kappa + S_e/d_0^2. \tag{25b}$$

Equation (25a) follows from full satisfaction of the interface boundary condition (14a) by $Z_0(0)$ itself, while (25b) follows from the additional physics brought by downstream amplitude change and basic state cross-flow.

The boundary condition (25b) implies $X_1(x) = O(1)$, while (12a, b) imply that Y_1 and Z_1 are $O(k)$. Thus, expanding X_1 as

$$X_1(x) = X_1^{(0)}(x) + k^2 X_1^{(1)}(x) + \cdots,$$

and inserting it in (12c), the downstream momentum equation, gives to $O(1)$ in k^2:

$$-\left(1 + \frac{d\bar{v}}{dx}\right) X_1^{(0)} = \kappa(\bar{v} Y_0^{(0)} + Z_0^{(0)}) + \frac{S_e}{\bar{d}} \frac{dY_0^{(0)}}{dx}.$$

After substitution for the $F = 0$ variables, one finds

$$X_1^{(0)}(x) = \left(\kappa + \frac{S_e}{\bar{d}^2}\right) e^{-x}. \tag{26}$$

This satisfies the boundary condition (25b) identically.

Solutions for Y_1 and Z_1 may now be obtained to lowest order in k^2 from (12a, b). With

$$Y_1 = kS(x), \quad Z_1 = kT(x),$$

one may substitute for X_1 from (26) and eliminate S in favor of T to obtain

$$\frac{d^2T}{dx^2} - T = 2\kappa e^{-x}(2\bar{v} + 1). \tag{27}$$

Using the boundary condition $T(0) = 0$ from (25a), one may solve this to give

$$T(x) = \kappa e^{-x}\left(\frac{4}{3}\bar{v} - \frac{4}{3}v_0 - x\right), \tag{28}$$

which, in turn, yields,

$$S(x) = \kappa e^{-x}\left(\frac{4}{3}v_0 - \frac{2}{3}\bar{v} - 1 + x\right) - \frac{S_e}{\bar{d}}e^{-x}. \tag{29}$$

To close the $O(F)$ system for κ, one must continue the solutions to $O(k^2)$. Evaluating the downstream momentum equation (12c) to this order gives

$$\bar{d}X_1^{(1)}(x) = \bar{v}S + T - \kappa\bar{v}Y_0^{(1)} - \kappa Z_0^{(1)} - \frac{S_e}{\bar{d}}\frac{dY_0^{(1)}}{dx}.$$

Here the right side is now completely known, except for κ. Evaluating this at $x = 0$ and recognizing that $X_1^{(1)}(0) = 0$, since $X_1^{(0)}(0)$ already satisfies (25b), gives

$$\kappa = \frac{2S_e}{v_0(3 - 2v_0)}. \tag{30}$$

This is the principal result of this section and shows three primary features of the model wave growth. First, the sign of κ is the same as that of S_e. Thus, for $S_e = 1$, when there is basic state cross-flow away from the front (upward entrainment), the waves grow in the downstream direction, indicating instability; conversely for $S_e = -1$, when the cross-flow is toward the front (downward entrainment), the waves decay, indicating stability. Second, κ is independent of wavenumber so long as the waves are long; thus, there is no preferential or fastest growing unstable wave. Third, $\kappa = O(1)$, so that its dimensional counterpart from (10d) is

$$\kappa^* = F\kappa/\lambda,$$

much smaller than λ^{-1}, i.e., the downstream growth scale will be $O(\lambda/F)$, many Rossby radii.

The best documented observations of growing frontal waves are those of the Gulf Stream downstream of Cape Hatteras. Hansen (1970) found $\kappa^* = (2 \pm 1) \times 10^{-3}$ km^{-1}, and Watts and Johns (1982) about 2.5 $\times 10^{-3}$ km^{-1}. Halliwell and Mooers (1983) analyzed the greatest amount of data for propagating, growing waves. For the frequency band $4 < \Omega < 8.5$ cpy they found $\kappa^* = (3.2 \pm 1.3) \times 10^{-3}$ km^{-1} with no perceptible variation with Ω. The model results sim-

ilarly show no change with Ω. For $v_0 = 1$ and $S_e = 1$, (30) gives $\kappa = 2$. Thus, for $\lambda = 27.8$ km, as in section 5, κ^* would match that of Halliwell and Mooers for $F = 0.044$, corresponding to a cross-stream flow into the parent pool of $u_t^* = Fc_i \cong 11$ cm s^{-1}, the order of magnitude one would expect. This value of κ^* corresponds to a downstream e-folding distance of 310 km, roughly comparable to the wavelength Λ predicted (Fig. 2) for this frequency band.

Further comprehension of the nature of wave amplitude growth or decay in the model is available through analysis of the wave kinetic energy. One may derive an equation describing this by first adding the product of (8) with $\bar{d}u'$ to the product of (9) with $\bar{d}v'$, then averaging the results over a wave period, and finally integrating over the entire inviscid domain. One finds

$$dK'/dt = R_{xy} + R_{xx} + A_K + W_P, \tag{31}$$

where

$$K' \equiv \int_0^\infty \frac{\bar{d}}{2}\langle u'^2 + v'^2\rangle dx,$$

the total wave or fluctuation kinetic energy,

$$R_{xy} \equiv \int_0^\infty \bar{d}\langle -u'v'\rangle \frac{d\bar{v}}{dx} dx,$$

the rate of working by wave cross-correlation Reynolds stress against basic state downstream velocity shear,

$$R_{xx} \equiv \int_0^\infty \bar{d}\langle -u'^2\rangle \frac{d\bar{u}}{dx} dx,$$

the rate of working by wave autocorrelation Reynolds stress against basic state cross-stream current gradient,

$$A_K \equiv \frac{d_0}{2}\bar{u}(0)\langle(u'^2 + v'^2)|_{x=0}\rangle,$$

the net advection of wave kinetic energy by basic state cross-stream volume flux, and

$$W_P \equiv \int_0^\infty \bar{d}\left\langle -u'\frac{\partial d'}{\partial x} - v'\frac{\partial d'}{\partial y}\right\rangle dx,$$

the rate of working by wave pressure gradient forces. The angle brackets here denote quantities averaged over a wave period. The terms on the right of (31) may be computed by taking the real parts of the products of the fluctuating properties involved and using the wave forms and subsequent expansions in k^2 and F:

$$R_{xy} = S_e F\gamma\left[\frac{4 - 3v_0}{6(3 - 2v_0)} + v_0^{-2}\log d_0^{-1} - v_0^{-1} - \frac{1}{2}\right],$$

$$R_{xx} = O(k^2F),$$

$$A_K = S_e F\gamma/2,$$

$$W_P = -S_e F\gamma(v_0^{-2}\log d_0^{-1} - v_0^{-1}),$$

where $\gamma = \frac{1}{2}\exp(2Fky)$, the amplitude growth factor. Thus, in the next kinetic energy production expressed by the right side of (31), R_{xx} is negligible while the other three terms are $O(F)$. Here R_{xy} has the sign of S_e for $0 < v_0 < 1$ so that this Reynolds stress term extracts energy from the basic state flow for $S_e = 1$ but supplies it for $S_e = -1$. The log singularity for $d_0 \rightarrow 0$ reflects the singularity in $\bar{u}(0)$ for that limit. The advection of wave kinetic energy likewise has the sign of S_e, but the pressure gradient work term has the opposite sign. In summing these terms the two log-singularity terms cancel and the net result is simply the first term of R_{xy}:

$$dK'/dt = \frac{(4 - 3v_0)}{6(3 - 2v_0)} S_e F\gamma. \qquad (32)$$

Consequently, wave kinetic energy growth or instability occurs with $S_e = 1$, and decay with $S_e = -1$, consistent with the result (30) for wave amplitude growth κ. For the limiting case $v_0 \rightarrow 1$ ($d_0 \rightarrow 0$), one has simply

$$dK'/dt = S_e \frac{F\gamma}{6} = \frac{Fk\gamma}{12}.$$

In the net production or decay of wave kinetic energy, then, the wave cross-correlation Reynolds stress $\langle -u'v' \rangle$ plays the critical role, as one would expect from a model with only one active layer ("barotropic"). To $O(F)$ and lowest order in k^2 one may write the fluctuation product as

$$-u'v' = -2\gamma(X_0^{(0)}Y_0^{(0)}\sin\alpha\,\cos\alpha + FY_0^{(0)}X_1^{(0)}\cos^2\alpha),$$

where $\alpha \equiv ky - \omega t$. The time mean of the first term on the right vanishes because its harmonic functions are in quadrature phase, i.e., the quadrature phase between u' and v' in the $F = 0$ flow can produce no Reynolds stress. However, the $O(F)$ flow alters this phase, as the $O(F)$ terms in the wave forms (10a, b) for u' and v' show. In consequence, the second term above produces the time mean Reynolds stress of $O(F)$ that, in turn, accounts for the net production or loss of wave kinetic energy.

7. Concluding remarks

In this paper I have developed a simple, analytic model of small amplitude, long, free wave disturbances to an established upper ocean density front. The major characteristic of the model is the structure of the basic state assumed, essentially Stommel's (1966) model of the Gulf Stream in deep water where the active, upper layer has uniform potential vorticity. Two major categories of frontal wave dynamics result; the slow, downstream propagation of long waves which are stable in the absence of basic state cross-stream flow ($F = 0$), and modified forms of these which grow or decay downstream in the presence of small basic state cross-flow ($0 < F \ll 1$). The model fits within the general class of barotropic models, as

it has only one active layer, but falls outside the class of quasi-geostrophic models, as the basic state current has a Rossby number $O(1)$. It may be viewed as an extension of G83 for the long wave or zeroth mode obtained by relaxing the condition of no shear across the inner boundary.

The major properties of the waves for $F = 0$ are 1) phase and group speeds which are much slower than the basic state downstream current, 2) phase speeds which increase with the wavenumber squared or with the frequency to the two-thirds power, and 3) anomalous dispersion. To lowest order in k^2 the cross-stream momentum balance for the waves is geostrophic and potential vorticity changes are suppressed by a simple balance between perturbations in lateral shear of the downstream current and interface depth. In the wave troughs, where the current is faster, the interface shoals, and the reverse obtains for the crests: Properties which should be readily observable. The downstream momentum balance, in contrast, is neither simple nor geostrophic, but contains both downstream and cross-stream advection of momentum, as well as the geostrophic terms. For the limiting case of no dissipative zone ($d_0 \rightarrow 0$) the lowest order results agree with those of Paldor (1982) for $k^2 \rightarrow 0$. They are also consistent with the model of Martin (1981). In application to Gulf Stream meanders the model gives phase speeds or wavelengths that agree over the long wave band with the results of Halliwell and Mooers (1983) based on satellite observations of propagating waves. Thus, even for as deep a flow as the Gulf Stream, one need not necessarily resort to two-layer or baroclinic models, such as Orlanski's (1969), to obtain similar wave properties to those observed.

A simple, barotropic long wave instability mechanism was found upon adding small cross-stream flow $\bar{u}$ to the basic state, such as would be driven by turbulent mass entrainment across the frontal interface within the narrow dissipative zone. The mechanism differs fundamentally from that of classical barotropic instability in quasi-geostrophic models which require an extremum in basic-state potential vorticity. Here, in contrast, the potential vorticity is uniform. The model shows that wave amplitude and kinetic energy grow for cross-flow toward the parent pool, decay for the reverse, and are stable for zero cross-flow. The spatial rate of downstream amplitude growth is independent of wavenumber for long waves and has a downstream scale of $O(\lambda/F)$, many Rossby radii or frontal zone widths. Finite cross-flow eliminates the perfect quadrature phase found between u' and v' for $F = 0$ to yield small cross-correlation Reynolds stress $\langle -u'v' \rangle$ which works against the basic state shear of downstream velocity $d\bar{v}/dx$ to change wave kinetic energy. The results are consistent with those of Halliwell and Mooers (1983), especially in the lack of dependence of spatial growth rate on wavenumber.

The primary object of the model is to illuminate basic frontal wave mechanisms and to suggest approaches for more sophisticated models, especially numerical ones. The latter, in particular, should permit full coupling of a dissipative inner zone structure, such as a time-dependent version of Assaf's (1977) model, with a nearly inviscid outer zone. In addition, they might treat other potentially important complications, necessarily omitted here, such as finite amplitude waves and downstream variation in the basic state, simulating, for example, progressive departure of volume flux from the Gulf Stream into the interior, recirculation region.

REFERENCES

Assaf, G., 1977: The Gulf Stream: Inertia and friction. *Tellus,* **29,** 137–143.

Garvine, R. W., 1974: Dynamics of small-scale oceanic fronts. *J. Phys. Oceanogr.,* **4,** 557–569.

——, 1980: The circulation dynamics and thermodynamics of upper ocean density fronts. *J. Phys. Oceanogr.,* **10,** 2058–2081.

——, 1983: Stationary waves on oceanic density fronts. *Deep Sea Res.,* **30,** 245–266.

Halliwell, G. R., and C. N. K. Mooers, 1983: Meanders of the Gulf Stream downstream from Cape Hatteras 1975–1978. *J. Phys. Oceanogr.,* **13,** 1275–1292.

Hansen, D. V., 1970: Gulf Stream meanders between Cape Hatteras and the Grand Banks. *Deep Sea Res.,* **17,** 495–511.

Johns, E. M., and D. R. Watts, 1982: An analysis of the potential vorticity distribution across the Gulf Stream. *Proc. Workshop Gulf Stream Variability,* Research Triangle Park, NC, 153–163.

Kao, T. W., 1980: The dynamics of ocean fronts. Part I: The Gulf Stream. *J. Phys. Oceanogr.,* **10,** 483–492.

——, C. Park and H.-P. Pao, 1977: Buoyant surface discharge and small-scale oceanic fronts: A numerical study. *J. Geophys. Res.,* **82,** 1747–1766.

Martin, W. W., 1981: Oceanic frontal stability: A numerical model. Ph.D. dissertation, University of Delaware, 136 pp.

McDowell, S., P. Rhines and T. Keffer, 1982: North Atlantic potential vorticity and its relation to the general circulation. *J. Phys. Oceanogr.,* **12,** 1417–1436.

Orlanski, I., 1969: The influence of bottom topography on the stability of jets in a baroclinic fluid. *J. Atmos. Sci.,* **26,** 1216–1232.

Paldor, N., 1982: Stable and unstable modes of surface fronts. Ph.D. dissertation, University of Rhode Island, 62 pp.

Rhines, P. B., and W. R. Young, 1982a: Homogenization of potential vorticity in planetary gyres. *J. Fluid Mech.,* **122,** 347–367.

——, and ——, 1982b: A theory of wind-driven circulation. *J. Mar. Res.,* **40** (Suppl.), 559–596.

Stommel, H., 1966: *The Gulf Stream.* University of California Press. 248 pp.

Watts, D. R., and W. E. Johns, 1982: Gulf Stream meanders: Observations on propagation and growth. *J. Geophys. Res.,* **87,** 9467–9476.